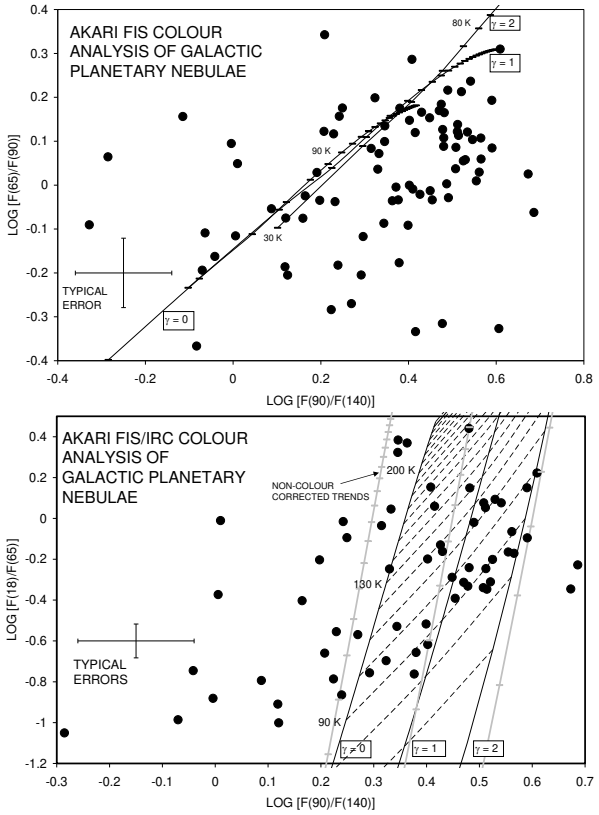

Fig. 5. Positions of PNe in the FIS/IRC colour-colour planes (filled circles), together with diagonal lines corresponding to colour-corrected grain emission loci. The temperatures of the grains are indicated by ticks and dashed lines, and represent increments of 10 K in $T_{\rm GR}$. Similarly, the diagonal loci correspond to emissivity exponents γ = 0, 1, and 2, as indicated in the panels. Finally, we have indicated the mean errors in the colours (error bars to the left-hand side), and the effects of not including colour corrections (the grey diagonal lines in the lower panel). Note that whilst a large fraction of PNe in the lower panel fall within the limits of the dust continuum loci, this is less the case in the upper panel, where most of the nebulae are positioned to the right. Some of these disparities are attributable to errors in the results, and to the contribution of line and band components.

tailed analysis of sources in which the continuum is clearly visible, and the S/N is reasonably high, suggests that [OIV] λ25.87 makes the largest average contribution to the 18 μm band ($\sim$20% of the dust continuum flux), whilst total line enhancement is of the order $\sim$40%. The line contributions to the other channels are less substantial, varying from $\sim$13% (at 65 μm), to $\sim$7% (90 μm), $\sim$0.4% (140 μm) and 4% (160 μm, where [CII] is strongest). Given the nature of the colour-colour mapping to be discussed in § 3.2, it is relevant to note that mean 18 μm/65 μm flux ratios would be increased by $\sim$22% (i.e. points would be shifted by $\sim$0.09 dex), whilst corrections to the other ratios are significantly less.

Finally, of the 32 PNe investigated in this present analysis, nine appear to have strong 30 μm features. These mostly fall between the IRC 18μm filter on the one hand, and the FIS 65 and 90 μm filters on the other. Their contributions to the AKARI photometry are therefore likely to be modest.

Some care must therefore be taken in interpreting the present photometry – a caveat that also applies to previous such analyses. Thus for instance, the analysis of Pottasch et al. (1984) is similar to that we shall be undertaking below, although the authors appear not to have taken account of colour corrections. Stasinska & Szczerba (1999) have attempted a more sophisticated analysis, in which photometry is corrected using SED evolutionary modeling. The authors ignore several important oxygen- and carbon-rich bands, however, whilst their assumptions of invariant abundances, identical nebular structures, a single grain emissivity function, and various other approximations, may lead to misleading results for many of their sample PNe.

3.2. *The AKARI Colour-Colour Planes, and Variation of Grain Temperatures*

The distribution of PNe within the AKARI colour planes is illustrated in Figure 5, where the upper panel shows trends with respect to the 65 μm/90 μm and 90 μm/140 μm flux ratios, and the lower panel represents the corresponding 18 μm/65 μm–90 μm/140 μm ratios. We also indicate the trends to be expected for smooth dust continua having emissivity exponents γ = 0, 1 and 2, and temperatures 30 K $< T_{\rm GR} <$ 270 K. The errors in the fluxes have been discussed in § 2.2, where it is noted that PNe with $F_\nu(18\mu{\rm m}) > 1$ Jy have S/Ns $\sim$15. Similar values apply for the FIS photometric results as well, where combined relative errors of $\sim$10%, and absolute errors of $\sim$15% lead to overall photometric uncertainties of $\sim$20%. We have used these estimates in determining the error bars in Figure 5.

A further correction relates to the broad widths (4.8–52.4 μm) of the AKARI filters, which necessitates a modification to the fluxes depending upon the nature of the SEDs. We have used the colour corrections of Shirahata et al. (2009) and Lorente et al. (2007) to modify the dust continuum trends in Figure 5, leading to shifts in the loci by as much as $\sim$0.1 dex. This leads to an overlapping of loci in